Chemistry–A European Journal
Research Article
doi.org/10.1002/chem.202302964
Chemistry Europe
European Chemical Societies Publishing
www.chemeurj.org

Special Collection

Controllable Structural Transformation of Non-Porous Propyl-Malonate Hexakis[60]fullerene by Chloroform Uptake/Release

Estefanía Fernández-Bartolomé,[a, b] José Santos,[b] Eider Rodriguez-Sánchez,[b] E. Carolina Sañudo,[c, d] Nazario Martín,*[a, b] and José Sánchez Costa*[a]

The design of dynamic structures with high recognition host-guest materials capable to host selectively small volatile molecules is an emergent field of research with both fundamental and applied implications. The challenge of exploring novel materials with advanced functionalities has led to the development of dynamic crystalline structures promoted by soft interactions. Here, a new pure organic dynamic framework based on hexakis[60]fullerene that are held together by weak van der Waals interactions is described. This crystalline structure is capable of absorbing and releasing chloroform, through internal structural reorganization. This research provides new insight into the design of organic molecular crystals for selective adsorption applications.

Introduction

Engineered organic molecular crystals are steadily gaining attention in the adsorption field, where conventionally nanoporous materials are playing a leading role.[1] Compared to COFs and MOFs, which commonly tend to contain pores in their crystal structures[2–7] direct assembly of discrete organic molecules giving rise to porous structures is challenging. Generally, they tend to pack efficiently to maximize attractive intermolecular contacts and minimize voids in the crystal lattice, giving rise to stable assemblies.[8] In the absence of a porous layout, the uptake/loss of the host is also possible. In this case, the diffusion through the crystal lattice is facilitated by its dynamism, where intermolecular bonds may rearrange to favourably accommodate the host.[9–12]

The detection and control of volatile organic compounds (VOCs), including chloroform, has become increasingly important due to their harmful effects on the environment and human health.[13,14] Chloroform is a common VOC emitted from various sources, such as industrial processes and water chlorination, being classified as a probable human carcinogen by the International Agency for Research on Cancer[15] Therefore, dynamic structures formed through supramolecular interactions between molecules offer a promising alternative for absorbing chloroform and other VOCs emitted from natural and man-made sources.

Our research group recently reported on a novel and promising family of pure molecular dynamic crystalline frameworks that are held together by weak CH···HC van der Waals interactions[16], marking the first time such interactions have been reported in this field.[17,18] In this study, the fullerene-based organic material exhibited a non-porous dynamic crystalline structure capable of undergoing single-crystal-to-single-crystal (SCSC) topochemical reactions,[19] that resulted in colour change upon exposure to VOCs and thermal phase transition. Previous attempts to use these materials (C_{60} hexaaduct frameworks) as supramolecular host-guest systems revealed only Henry behaviour and no microporosity upon activation of the potential pores of the compounds was observed.[20] As a result, the challenge of crystallizing stable fullerene structures possessing porosity or demonstrating the ability to incorporate molecules through internal structural reorganization (breathing effect) remains challenging.

In this work, a crystalline non-porous dynamic organic molecule connected by supramolecular van der Waals inter-

[a] Dr. E. Fernández-Bartolomé, Prof. Dr. N. Martín, Dr. J. Sánchez Costa
IMDEA
Nanociencia C/Faraday 9
Ciudad Universitaria de Cantoblanco
28049 Madrid (Spain)
E-mail: jose.sanchezcosta@imdea.org
nazmar@quim.ucm.es
Homepage: http://www.imdeananociencia.org/switchable-nanomaterials/home

[b] Dr. E. Fernández-Bartolomé, Dr. J. Santos, Dr. E. Rodriguez-Sánchez, Prof. Dr. N. Martín
Departamento de Química Orgánica
Facultad de Ciencias Químicas
Universidad Complutense
28040 Madrid (Spain)
E-mail: nazmar@quim.ucm.es
Homepage: http://www.nazariomartingroup.com/

[c] Dr. E. C. Sañudo
Departament de Química Inorgànica i Orgànica
Secció de Química Inorgànica
Universidad de Barcelona
C/Martí i Franqués 1–11, 08028 Barcelona (Spain)

[d] Dr. E. C. Sañudo
Institut de Nanociència i Nanotecnologia
Universitat de Barcelona (IN2UB)
C/Martí i Franqués 1–11, 08028 Barcelona (Spain)
Homepage: https://webgrec.ub.edu/webpages/000007/cas/esanudo.ub.edu.html

Supporting information for this article is available on the WWW under https://doi.org/10.1002/chem.202302964

Special Collection This article is part of a joint Special Collection in honor of Maurizio Prato.

actions based on hexakis[60]fullerene capable of uptaking/releasing chloroform molecules is reported. This purely organic non-porous material is capable of self-creating cavities to host (accommodate) chloroform molecules within its crystalline lattice. The release of interstitial chloroform from the crystal produces a reorganization of the crystal structure that results in changes in crystal symmetry. Notably, the starting structure is recovered upon recrystallization from chloroform. These transformations have been followed by single-crystal diffraction, which provides a direct observation of the molecular reorganization undergone within the lattice.

Results and Discussion

The propyl-malonate hexakis[60]fullerene (**1**) was synthesized using the Bingel–Hirsch cyclopropanation reaction[21,22], following the reported procedure that consists in the addition of dipropyl malonate to a C_{60} solution in chlorobenzene, with DBU used as a base (Figure 1). Simple purification by column chromatography affords a red-orange solid, identified as compound **1**.

Compound **1** can yield two distinct crystalline structures (**2** and **3**) depending on the solvent and crystallization method used. When the red-orange solid is crystallized from a mixture of chloroform and deuterated chloroform at room temperature by evaporation over two days, it provides orange crystals (**2**) suitable for X-ray diffraction. Alternatively, **1** may be crystallized from ethanol using the pressure tube technique[23], which results in large orange crystals (**3**) also suitable for X-ray diffraction analysis (see Figure 2).

Sample **2** crystallizes in the $R\bar{3}$ hexagonal space group (see Figure 2). The unit cell is comprised of ten fullerene hexaadducts arranged in four unequal layers, with an hexakis[60]fullerene located at each vertex of the polyhedron, which are shared by eight adjacent unit cells, and two fullerene molecules located in the centre of the cube. The fullerenes are surrounded by six chloroform molecules, with the chlorine atoms forming a lone pair-π interaction (Cl···O) and a hydrogen bond (C–H···O) with the oxygen atoms of the malonate groups of the enclosing fullerenes (see Figure 2).[24] Furthermore, the malonate moiety, which is in proximity to the chloroform molecule, forms an additional lone pair-π interaction with the adjacent hexakisfullerene's propyl branch, as depicted in Figure 2 and Figure S1. Finally, the vessels formed by the chloroform molecules are complete by a C–H···H–C interaction[25] involving three different fullerenes, as shown in Figure 2 and Figure S1. Notably, no evidence of any supramolecular π-π contact between neighbouring fullerene buckyballs may be observed in **2**, as previously reported.[17,18] The shortest distance between two adjacent layered fullerenes in **2** is measured to be 7.309 Å, which falls far beyond the range of supramolecular π–π interactions of pristine [60]fullerene.[26,27] Thus, no supramolecular interactions other than π-π are deemed to be the primary driving force for the packing of **2** (SI). Overall, these intermolecular forces lead to the formation of a stable and well-ordered crystal structure that is able to efficiently encapsulate and release chloroform molecules. In addition, compound **2** was exposed to other solvents in an attempt to exchange chloroform for other molecules (ethanol, methanol, water, acetone, acetic acid, formic acid, formaldehyde, acetonitrile), but the process was unsuccessful.

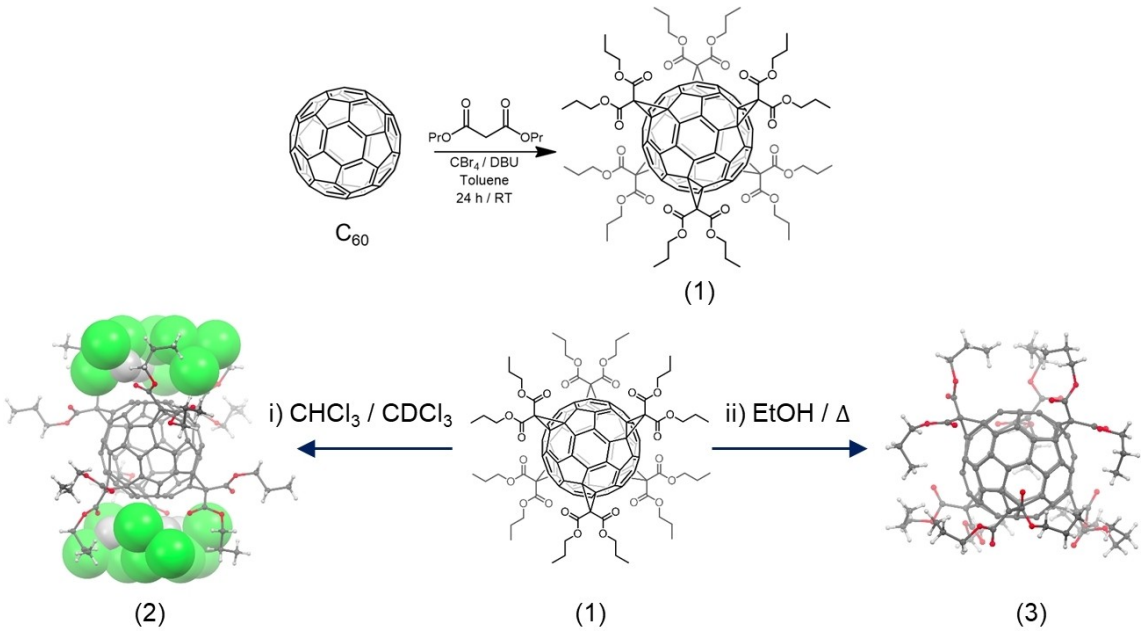

Figure 1. In top, synthesis of propyl-malonate hexakis[60]fullerene (**1**); Dipropyl malonate, toluene, 1,8-diazabicyclo[5.4.0]undec-7-ene (DBU), carbon tetrabromide (CBr_4). At the bottom, schematic crystallization conditions to achieve crystalline **2** and **3** from **1**. Single-crystal illustrations of samples **2** and **3** are displayed using MERCURY[21] software, with C atoms in gray, O atoms in red, Cl atoms in green, and H atoms in white.

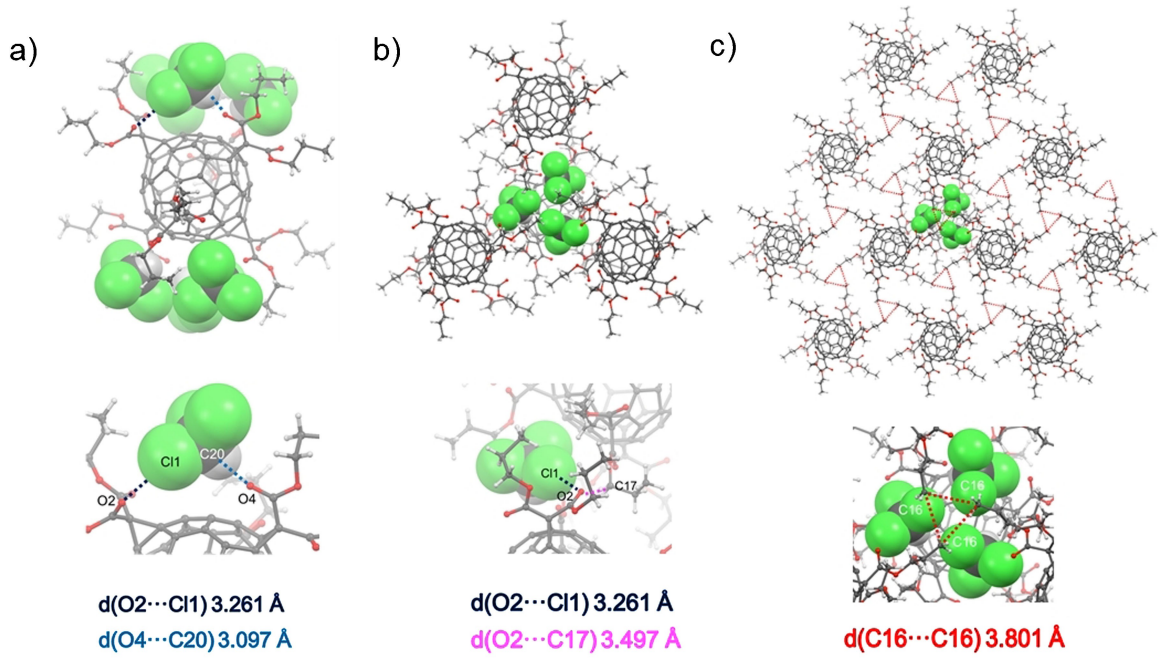

Figure 2. a) and b) illustrate the interactions between chlorine atoms of the chloroform molecules and the oxygen atom of the malonate group of the enclosing fullerene, with the main interaction highlighted in the amplifications shown below. c) displays the main intermolecular C···H–C contacts of **2** between adjacent alkyl branches of neighbouring fullerenes, with its amplification shown below.

Compound **3** exhibits a distinct crystal structure compared to **2**, as it crystallizes in the *F222* cubic space group. The asymmetrical unit of the crystal is comprised by two hexaadducts that are symmetry-equivalent but situated in two layers of unequal size. The conformation of the propyl malonate arms in **3** differs from that of **2**, as they are arranged in an open sideways fashion. This conformation allows the carbonyl groups to directly face the hydrogens of the adjacent fullerenes (Figure 3). As a result, the supramolecular packing in **3** is constructed through hydrogen bonds (C–H···O, Figure 3). Specifically, axial and lateral intermolecular interactions between adjacent fullerenes take place between oxygen atoms of

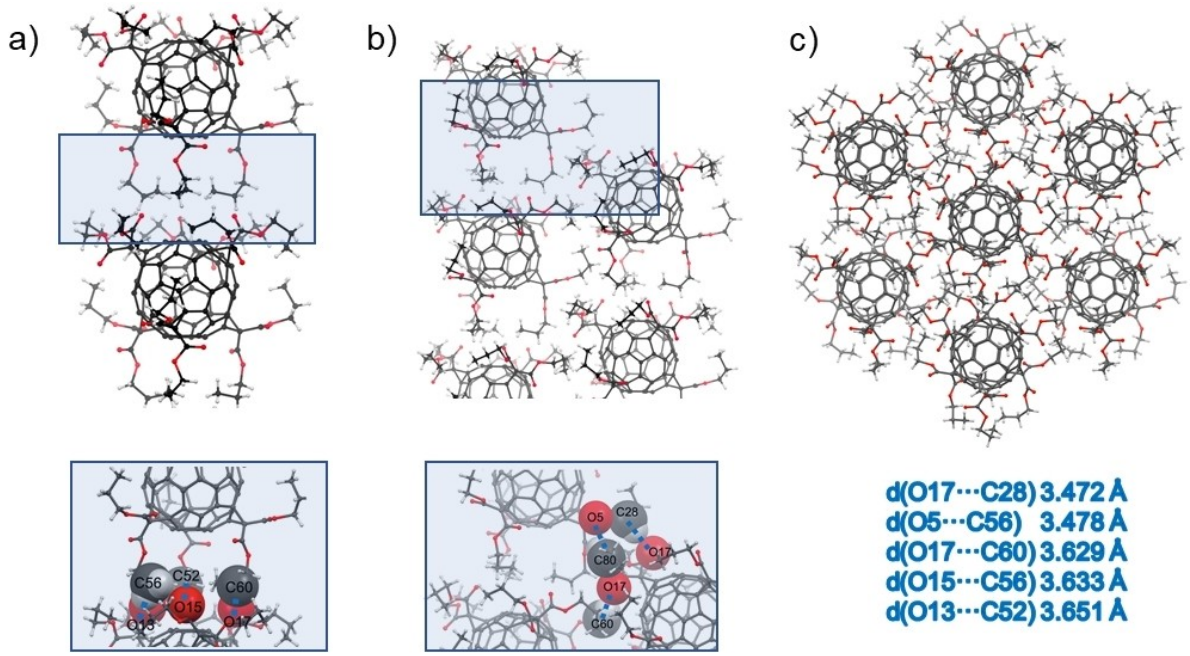

Figure 3. Depiction of the main connections along the whole packing in **3**, while panel a) and b) illustrate the C=O···H–C intramolecular interactions between carbonyl groups and propyl chains of adjacent fullerenes, with the principal interactions highlighted in the amplifications shown below, c) provides a view of the connections in the whole packing, with interactions omitted for clarity.

the carbonyl group of the malonate arms and the C2, C3, C1, C3 (regarding the carbonyl group) of adjacent alkyl branches, respectively (see Figure 3 and Figure S2). The minimum range of distance lengths goes from 3.260 to 3.303 Å and the maximum from 3.478 to 3.654 Å (for further information see Table S2). In this case, the shortest distance between two adjacent fullerenes situated in different layers is 7.76 Å, which is again completely outside the range of supramolecular π–π interactions.[26,27] Consequently, the supramolecular packing is only driven by hydrogen bonds (C–H···O).

Thermogravimetric (TG) analysis and optical reflectivity (OR) experiments shed light into the physico-thermal properties of both compounds (Figure S3, S4, S9 and S10 respectively). Thermogravimetric analysis (TGA) provides insights into the thermal stability of compound 2, which is stable up to 423 K, when it starts to decrease in weight composition (Figure S3). This is likely due to a decomposition process of the hexakis-fullerene. In contrast, compound 3 exhibits high stability, decomposing just above 540 K (Figure S4). This highly stability is attributed to the increased strain supported by a wide supramolecular network compared to sample 2.

Optical reflectivity experiments of **2** show three peaks at 300 K, 559 K, and 573 K during the heating ramp. The first peak at 300 K concurs with a variation in the brightness of the crystal and a significant change of size, and corresponds to a new phase (**2'**) with a size increase of 9.33 %. The peak at 559 K correlates with the beginning of the fusion of **2**, and no peaks are observed during the cooling ramp. Similarly, compound **3** is also analysed by optical reflectivity and exhibits two peaks (559 K and 563 K) corresponding to the onset of fusion, but the peak at 300 K, corresponding to the transition phase, is not observed.

To obtain detailed information on the composition of the new phase (**2'**), powder X-ray diffraction, single crystal X-ray diffraction (SC-XRD), and FTIR are carried out. SC-XRD is collected upon the exposure of **2** to air (at room temperature) for 30 minutes. After solving the crystal structure, it is found that the lattice parameters of **2'** are different from **2**, evidencing a phase transition. Furthermore, comparison between the lattice parameters of **2'** and **3** reveal that they are the same.

As illustrated in Figure 4, chloroform molecules are removed from **2** during exposure to air, leading to a transformation from a non-porous potential cavity structure to a more compact structure without solvent (**3**). Interestingly, sample **2** can be regenerated from **3** by recrystallization from chloroform (**3'**). The new transition phase, **2'**, is also monitored by FTIR spectroscopy (Figure S11), showing that the spectra of **2** and **2'** do not overlap, with the major difference occurring in the 900–700 cm^{-1} region, corresponding to the chloroform bands. The identical bands in both **2'** and **3** support the conclusion that they have the same structure and indicate that additional structural change takes place.

Conclusions

The work herein describes the first crystalline dynamic non-porous organic molecule based on hexakis[60]fullerene with the ability to trap/release solvent molecules. The large number of propyl branches of these fullerenes denote a dynamic interaction between interconnected aliphatic chains. In spite of being formally a non-porous compound, the flexibility provided by the dynamic structure allows the diffusion of volatiles into the crystal. Specifically, compound **2** exhibits potential cavities housing chloroform molecules within it. Chloroform molecules are carried away from **2** after exposure to air, resulting in a phase transformation, due to the reorganization of the propyl chains and their van der Waals contacts, from a non-porous potential cavity structure to a more compact solvent-free structure (**3**). The reorganization of the structure is also accompanied by a change in symmetry. Although this is not a reversible process, crystals of **2** can be recovered merely by recrystallization of **3**. Therefore, these structural changes can be directly visualized and followed by X-ray diffraction.

The design of novel functionalized hexaadducts of [60]fullerene will contribute to the creation of less-explored

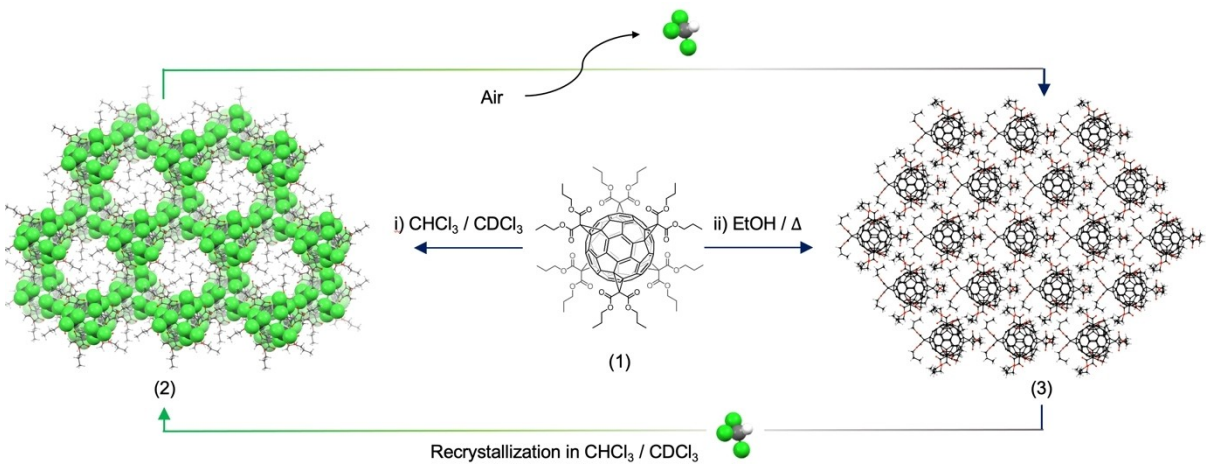

Figure 4. Release of chloroform molecules from **2** upon exposure to air giving rise to a transition from a potential nonporous cavity structure onto a compact solvent-free structure (**3**). Sample **2** can be recovered from **3** by recrystallization in chloroform.

innovative and dynamic advanced carbon-based materials, which pave the way to a variety of direct technological applications, such as adsorption and exchange for many other analytes.

Experimental Section

The experimental details are described in the supporting section.

Physical measurement

NMR spectra were recorded on a Bruker Advance 300 (1H: 400 MHz) spectrometer at 298 K using partially deuterated solvents as internal standards. Coupling constants (J) are denoted in Hz and chemical shifts (δ) in ppm. Multiplicities are denoted as follows: s = singlet, d = doublet, t = triplet, m = multiplet.

FT-IR spectra were recorded as neat samples in the range 400–4000 cm^{-1} on a Bruker Tensor 27 (ATR device) Spectrometer.

TGA was performed using a TA Instrument TGAQ500 with a ramp of 2 °C/min under air and nitrogen from 30 to 500 °C.

Mass spectra Matrix assisted Laser desorption ionization (coupled to a Time-of-Flight analyzer) experiments (MALDI-TOF) were recorded on a MAT 95 thermo spectrometer and a Bruker REFLEX spectrometer respectively.

Crystal Structure Determination: The data were collected with an orange block crystal of 2 and 2 h with a MD2 M-Maatel diffractometer at the XALOC beamline (BL13) at ALBA Synchrotron with the collaboration of ALBA staff, from a Silicon (111) monochromator (T = 100 K, λ = 0.82656 Å). The crystal was taken directly from its solution, mounted with a drop of Paratone-N oil and immediately put into the cold stream of dry N_2 on the goniometer. The structure was solved by direct methods and the refinement on F_2 and all further calculations were carried out with the SHELX-TL suite and OLEX2 program. The CCDC number are included in the crystal data table (see SI1 and Table S1).

Optical reflectivity measurements between 288 and 373 K were performed using a MOTIC SMZ-171 optical stereoscope coupled with a MOTICAM 3. Images were collected in BMP format without any filter using the Motic Images Plus 3.0 software, with the mean value from each region of interest (ROI) analyzed under the ImageJ program. The temperature was controlled using a Linkam T95 system controller and a LNP 95 Liquid Nitrogen Cooling System.

Synthesis of 1, 2 and 3

Sample **1**: A mixture of dipropyl malonate (0.3 g, 1.39 mmol), C60 (100 mg, 0.139 mmol) and CBr4 (0.46 g, 1.39 mmol) in toluene (50 mL) is stirred at room temperature until the fullerene is dissolved. Then DBU (0.414 mL, 2. 78 mmol) is added dropwise and the mixture is stirred for 24 h at room temperature. The reaction is stopped by adding water (50 mL) and the organic phase is separated, dried with Na_2SO_4, filtered and the solvent is removed under reduced pressure. The resulting crude is purified by column chromatography (silica gel; CS2/EtOAc) to afford a red-orange solid (160 mg, 0.086 mmol, 62%). 1H-NMR ($CDCl_3$, 400 MHz, 298 K): δ/ppm 4.24 (t, J = 6.7 Hz, 24H), 1.74 (m, 24H), 0.96 (t, J = 7.4 Hz, 36H) ppm (Figure S5). 13 C-MR ($CDCl_3$, 100 MHz, δ): 163.9, 145.7, 141.2, 69.1, 66.4, 45.5, 21.8, 10.3 ppm (Figure S6).; MS.(MALDI TOF): m/z calc. for [M + 1] 1837.508 (Figure S7).

Sample **2**: 10 mg of hexakis adduct fullerene were dissolved in chloroform and deuterated chloroform at room temperature and put in a screw vial for chromatography (diameter 12 mm, height 32 mm). The orange cube-shaped crystals (**2**) suitable for X-ray diffraction were obtained by evaporation 2 days after.

Sample **3**: 10 mg of hexakis adduct fullerene were dissolved in EtOH (12 mL) in a pressure tube (diameter 27 mm, height 55 mm). The tube was sealed and kept at 120 °C for 3 days in a furnace. A week after, orange needle-shaped crystals suitable for X-ray diffraction analysis, were obtained (**2**) (8 mg, 80%).

Deposition Numbers 2266752 (for 3'), 2266753 (for 2), 2266754 (for 3) and 2266755 (for 2') contain the supplementary crystallographic data for this paper. These data are provided free of charge by the joint Cambridge Crystallographic Data Centre and Fachinformationszentrum Karlsruhe Access Structures service.

Acknowledgements

JSC thanks funds from the Spanish MICINN through National Research Project (AIRE PID2019-111479GB-I00, PID2020-114653RB-I00 and TED2021-131018B-C22) and the MAD2D-CM-MRR MATERIALES AVANZADOS-IMDEANC4 and MAD2D-CM-MRR-UCM-1. EFB thanks the *Juan de la Cierva Formación* (FJC2021-047249-I) grant. IMDEA Nanociencia acknowledges support from the 'Severo Ochoa' Programme for Centres of Excellence in R&D (MINECO, Grant CEX2020-001039-S), the NANOMAGCOST (P2018/NMT4321). ECS acknowledges financial support by Spanish MCINN (project PGC2018-098630-B-I00). We thank the XALOC-ALBA synchrotron source under project 2023017235.

Conflict of Interests

The authors declare no conflict of interest.

Data Availability Statement

The data that support the findings of this study are available from the corresponding author upon reasonable request.

Keywords: chloroform uptake/release · crystal engineering · fullerene · non-porous acting as porous · single crystal diffraction · Van der Waals contact

[1] M. E. Casco, F. Krupp, S. Grätz, A. Schwenger, V. Damakoudi, C. Richert, W. Frey, L. Borchardt, *Adsorption* **2020**, *26*, 1323–1333.
[2] J. L. C. Rowsell, O. M. Yaghi, *Microporous Mesoporous Mater.* **2004**, *73*, 3–14.
[3] Z. Mu, Y. Zhu, B. Li, A. Dong, B. Wang, X. Feng, *J. Am. Chem. Soc.* **2022**, *144*, 5145–5154.
[4] H. Furukawa, K. E. Cordova, M. O'Keeffe, O. M. Yaghi, *Science* **2013**, *341*, 12304445.
[5] A. P. Cote, A. I. Benin, N. W. Ockwig, M. O'Keeffe, A. J. Matzger, O. M. Yaghi, *Science* **2005**, *310*, 1166–1171.
[6] A. Gamonal, C. Sun, A. L. Mariano, E. Fernandez-Bartolome, E. Guerrero-Sanvicente, B. Vlaisavljevich, J. Castells-Gil, C. Marti-Gastaldo, R. Poloni,

R. Wannemacher, J. Cabanillas-Gonzalez, J. Sanchez Costa, *J. Phys. Chem. Lett.* **2020**, *11*, 3362–3368.
[7] N. Alegret, A. Dominguez-Alfaro, J. M. González-Domínguez, B. Arnaiz, U. Cossío, S. Bosi, E. Vázquez, P. Ramos-Cabrer, D. Mecerreyes, M. Prato, *ACS Appl. Mater. Interfaces* **2018**, *10*, 43904–43914.
[8] J. L. Atwood, L. J. Barbour, A. Jerga, B. L. Schottel, *Science* **2002**, *298*, 1000–1002.
[9] E. Resines-Urien, E. Burzurí, E. Fernandez-Bartolome, M. Á. García García-Tuñón, P. De La Presa, R. Poloni, S. J. Teat, J. Sanchez Costa, *Chem. Sci.* **2019**, *10*, 6612–6616.
[10] S. Rodríguez-Jiménez, H. L. C. Feltham, S. Brooker, *Angew. Chem. Int. Ed.* **2016**, *55*, 15067–15071.
[11] E. Fernandez-Bartolome, E. Resines-Urien, M. Murillo-Vidal, L. Piñeiro-Lopez, J. Sánchez Costa, *Inorg. Chem. Front.* **2021**, *8*, 2426–2432.
[12] J. Sanchez Costa, S. Rodríguez-Jiménez, G. A. Craig, B. Barth, C. M. Beavers, S. J. Teat, G. Aromí, *J. Am. Chem. Soc.* **2014**, *136*, 3869–3874.
[13] S. Li, Y. Lin, G. Liu, C. Shi, *Environ. Sci. Process. Impacts* **2023**, *25*, 727–740.
[14] E. Resines-Urien, L. Piñeiro-López, E. Fernandez-Bartolome, A. Gamonal, M. Garcia-Hernandez, J. Sánchez Costa, *Dalton Trans.* **2020**, *49*, 7315–7318.
[15] http://www.iarc.who.int (accessed 22 May 2023).
[16] H. L. Hou, C. Anichini, P. Samorì, A. Criado, M. Prato, *Adv. Funct. Mater.* **2022**, *32*, 2207065.
[17] E. Fernandez-Bartolome, J. Santos, A. Gamonal, S. Khodabakhshi, L. J. McCormick, S. J. Teat, E. C. Sañudo, J. S. Costa, N. Martín, *Angew. Chem. Int. Ed.* **2019**, *58*, 1310–2315.
[18] E. Fernandez-Bartolome, A. Gamonal, J. Santos, S. Khodabakhshi, E. Rodríguez-Sánchez, E. C. Sañudo, N. Martín, J. Sánchez Costa, *Chem. Sci.* **2021**, *12*, 8682–8688.
[19] E. Fernandez-Bartolome, A. Martinez-Martinez, E. Resines-Urien, L. Piñeiro-Lopez, J. Sánchez Costa, *Coord. Chem. Rev.* **2022**, *452*, 214281.
[20] A. Kraft, C. Roger, D. Schmidt, J. Stangl, K. Müller-Buschbaum, F. Beuerle, *Chem. Eur. J.* **2017**, *23*, 15864–15868.
[21] C. Bingel, *Chem. Ber.* **1993**, *126*, 1957–1959.
[22] I. Lamparth, C. Maichle-Mössmer, A. Hirsch, *Angew. Chem. Int. Ed.* **1995**, *34*, 1607–1609.
[23] Y. Huo, S. Xiu, L. Y. Meng, B. Quan, *Chem. Eng. J.* **2023**, 451.
[24] J. P. M. Lommerse, A. J. Stone, R. Taylor, F. H. Allen, *J. Am. Chem. Soc.* **1996**, *118*, 3108–3116.
[25] J. Echeverría, G. Aullón, D. Danovich, S. Shaik, S. Alvarez, *Nat. Chem.* **2011**, *3*, 323–330.
[26] A. O'Neil, C. Wilson, J. M. Webster, F. J. Allison, J. A. K. Howard, M. Poliakoff, *Angew. Chem. Int. Ed.* **2002**, *41*, 3796–3799.
[27] M. V. Korobov, A. L. Mirakian, N. V. Avramenko, E. F. Valeev, I. S. Neretin, Y. L. Slovokhotov, A. L. Smith, G. Olofsson, R. S. Ruoff, *J. Phys. Chem. B* **1998**, *102*, 3712–3717.

Manuscript received: September 13, 2023
Accepted manuscript online: October 17, 2023
Version of record online: November 16, 2023